JOURNAL OF SOLID STATE CHEMISTRY 56, 325–334 (1985)

High-Temperature Redox Behavior of Doped $SrTiO_3$ and $LaCrO_3$

H. U. ANDERSON, M. M. NASRALLAH,* B. K. FLANDERMEYER, AND A. K. AGARWAL

Department of Ceramic Engineering, University of Missouri-Rolla, Rolla, Missouri 65401

Received November 30, 1983; in final form July 27, 1984

The stability of high-temperature fuel cell electrodes to their ambient environment is important for the long-term reliability of fuel cells. In this report the behavior of oxide electrode materials as a function of oxygen activity and temperature is considered. Models for the oxidation–reduction behavior of both *p*- and *n*-type oxides are presented. These models take into account the absorption and evolution of oxygen which take place as oxygen activity is varied. The resulting instability in electrical conductivity is explained as a consequence of changes in carrier concentration due to variability in ionic defect concentration. The proposed models are applied to acceptor-doped $LaCrO_3$ and donor-doped $SrTiO_3$. It is shown that the models explain the experimental data well and as a consequence diagrams can be made which show the regions of oxygen activity and temperature for which stability of electrical conductivity and defect structure might be expected.

I. Introduction

For long-term reliability of fuel cells, it is essential that the electrodes used be stable, both electrically as well as structurally, at elevated temperatures in the presence of the required electrolytes and varying oxygen activities. A number of oxides are candidates for this application with some of the most promising being from the perovskite family. For many of the ABO_3 compounds, sufficient electrical conductivity is obtainable by substitution on either the *A* or *B* sites, by acceptor- or donor-type cations; depending on the intrinsic defect structure of the parent oxide. However, it is known that under certain oxygen activity conditions the electrical conductivity can decrease such that the material becomes unsuitable as an electrode.

It is the purpose of this report to show how the defect structure and electrical conductivity change as perovskite-type oxides equilibrate under various oxygen activities at elevated temperatures. Models for the oxidation–reduction behavior of both *n*- and *p*-type oxides are presented. The models are applied to acceptor-doped $LaCrO_3$, and donor-doped $SrTiO_3$. The proposed models are verified by electrical conductivity and thermogravimetric measurements as a function of oxygen activity and temperature. The experimental results are used to construct Kröger–Vink-type diagrams showing the stability regimes for both oxides.

Strontium titanate is known (*1–3*) to be

* Currently on leave from Faculty of Engineering, Cairo University, Egypt.

0022-4596/85 $3.00

a *n*-type oxide by formation of oxygen vacancies. Lanthanum-doped $SrTiO_3$ shows a reversible weight loss upon reduction (*4*), the weight loss was found to be directly proportional to the donor concentration. At higher P_{O_2} an uptake of stoichiometric excess of oxygen is observed. Since second phases have not been detected by either X-ray diffraction or electron microscopy, the absorbed oxygen has been accounted for by the presence of an as yet undetected crystallographic accomodation, possibly by the formation of "SrO" layers characteristic of the Ruddlesdon–Popper-type structure (*5*), these layers appear to be interleaved with the perovskite structure, leaving the oxygen sublattice intact. It is assumed that the donor dopant induces the absorption of oxygen which react to form the "SrO"-type layers and V''_{Sr} in the host lattice. Since the "SrO" layers are not considered a separate phase, the activity is not taken as unity but related to its corresponding mole fraction. The model developed for La-doped $SrTiO_3$ assumes that at lower P_{O_2} a controlled-valency-type compensation occurs by the formation of either Ti^{3+} or electrons in the conduction band whereas at higher P_{O_2} the donors are compensated by the formation of Sr vacancies, according to the reaction

$$Sr_{1-y-x}La_y^{\cdot}V''_{Sr_x}Ti'_{y-2x}Ti_{1-y+2x}O_3 + x\text{"SrO"} \underset{\text{red.}}{\overset{\text{oxid.}}{\rightleftharpoons}} Sr_{1-y}La_y^{\cdot}Ti'_yTi_{1-y}O_3 + x/2\ O_2 \quad (1)$$

where y represents the dopant concentration and x the excess oxygen. This reaction can be reduced to

$$\text{"SrO"} + 2Ti + V''_{Sr} \underset{\text{oxid.}}{\overset{\text{red.}}{\rightleftharpoons}} Sr + 2Ti' + \tfrac{1}{2}O_2(g). \quad (2)$$

Where $La^{\cdot}_{Sr}$ denotes La^{3+} on a substitutional Sr^{2+} site, Ti′ represents either an electron association with Ti^{4+} or an electron in the conduction band, and V''_{Sr} is an ionized Sr vacancy. The equilibrium constant for the reaction is given by

$$K_1 = \frac{[Sr][Ti']^2}{[SrO][Ti]^2[V''_{Sr}]} P_{O_2}^{1/2}. \quad (3)$$

If the assumption is made that the activities can be replaced by mole fraction of the respective terms and that "SrO" is not a separate phase but is due to structural accomodation which yields not only "SrO" but Sr vacancies then the expression for the equilibrium constant becomes

$$K_1 = \frac{(1 - y + x)(y - 2x)^2}{x^2(1 - y + 2x)^2} P_{O_2}^{1/2} \quad (4)$$

which with little loss in accuracy can be approximated to

$$K_1 = \frac{(y - 2x)^2}{x^2} P_{O_2}^{1/2}. \quad (5)$$

Rearrangement of this equation yields an expression for the excess oxygen as function of K_1 and P_{O_2}

$$x = \frac{yP_{O_2}^{+1/4}}{(K_1)^{1/2} + 2P_{O_2}^{1/4}}. \quad (6)$$

The electrical conductivity $\sigma = e\mu n$, where the carrier concentration $n = y - 2x$ can now be related to K_1 and P_{O_2}

$$\sigma = \frac{e\mu y(K_1)^{1/2}}{(K_1)^{1/2} + 2P_{O_{1/2}}^{1/4}}. \quad (7)$$

At low P_{O_2}, n approaches y and the amount of excess oxygen becomes

$$x = \frac{y}{(K_1)^{1/2}} P_{O_2}^{1/4}. \quad (8)$$

However, at high P_{O_2}, x approaches $y/2$, and

$$\sigma = \frac{e\mu y}{2} (K_1^{1/2})\, P_{O_2}^{-1/4} \quad (9)$$

and the relative conductivity at high P_{O_2} is given by

$$\sigma/\sigma_R = \frac{(K_1)^{1/2}}{2} P_{O_2}^{-1/4}, \quad (10)$$

where σ_R = conductivity when donors are compensated by electrons.

Lanthanum chromite, on the other hand, is known to be a *p*-type oxide (*6*) and becomes nonstoichiometric through the formation of cation vacancies. It is one of the promising materials for high-temperature electrode applications and fuel cell interconnects (*7*), however, volatilization and possibly corrosion impose certain limitations on the use of $LaCrO_3$. Several studies have been reported (*8–10*) relating its chemical stability and cation stoichiometry to volatilization and electrical conductivity.

The electrical conductivity of $LaCrO_3$ is essentially due to the 3*d* band of the Cr ions (*11*), thus an increase in conductivity is expected due to lower valence substitution on either the La^{3+} or Cr^{3+} sites resulting in the formation of Cr^{4+}. If such a substitution is compensated by the formation of oxygen vacancies, no additional contribution to the electronic conductivity is anticipated. The conditions under which equilibration of $LaCrO_3$ take place will determine whether electronic or ionic compensation will be favored. Even though densification requires a reducing atmosphere, the conductivity can be appreciably increased by subsequent equilibration in oxidizing atmosphere.

In this study Mg^{2+} was used as the acceptor dopant and assumed to enter the $LaCrO_3$ structure substitutionally for Cr^{3+}. Assuming *p*-type disorder in nonstoichiometric undoped $LaCrO_3$ and that all defects are fully ionized and the stoichiometric *A*/*B* ratio is maintained, the defect reaction under oxidizing and reducing conditions can be represented by

$$LaCr_{1-2y}Cr_y^{\cdot}Mg'_{Cr_y}O_3 \underset{\text{oxid.}}{\overset{\text{red.}}{\rightleftharpoons}} LaCr_{1-2y+x}Cr_{y-2x}^{\cdot}V_{o_x}^{\cdot\cdot}Mg'_{Cr_y}O_{3-x} + x/2\ O_2 \quad (11)$$

or

$$O_o + 2Cr_{Cr}^{\cdot} \leftrightarrows 2Cr_{Cr} + V_o^{\cdot\cdot} + \tfrac{1}{2}O_2. \quad (12)$$

The equilibrium constant for this reaction is given by

$$K_{11} = \frac{[Cr_{Cr}]^2[V_o^{\cdot\cdot}]}{[Cr_{Cr}^{\cdot}]^2[O_o]} P_{O_2}^{1/2} \quad (13)$$

and by substitution in terms of mole fraction

$$K_{11} = \frac{(1 - 2y + 2x)^2 x}{(y - 2x)^2(3 - x)} P_{O_2}^{1/2} \quad (14)$$

which can be approximated as

$$K_{11} = \frac{x}{(y - 2x)^2} P_{O_2}^{+1/2}. \quad (15)$$

The electrical conductivity $\sigma = e\mu p$, where the carrier concentration $p = y - 2x$, with which after solving Eq. (15) for x becomes

$$\sigma = \frac{e\mu}{4K_{11}} P_{O_2}^{1/2}[(8yK_{11}P_{O_2}^{-1/2} + 1)^{1/2} - 1]. \quad (16)$$

At the high P_{O_2} limit (x approaches zero) Eq. (16) reduces to $\sigma = e\mu y$, whereas, at low P_{O_2},

$$p = \left(\frac{y}{2K_{11}}\right)^{1/2} P_{O_2}^{1/4} \quad (17)$$

or

$$\sigma = e\mu \left(\frac{y}{2K_{11}}\right)^{1/2} P_{O_2}^{1/4} \quad (18)$$

and

$$\sigma/\sigma_R = \frac{P_{O_2}^{1/4}}{(2K_{11}y)^{1/2}}, \quad (19)$$

where σ_R is the conductivity when acceptors are compensated electronically.

II. Experimental

A series of La-doped $SrTiO_3$ and Mg-doped $LaCrO_3$ (0–20 at.%) compounds were prepared by the liquid mix process (*12*). In all cases stoichiometric *A*/*B* ratio was maintained, i.e., (Sr + La)/Ti or La/(Cr + Mg) = 1.

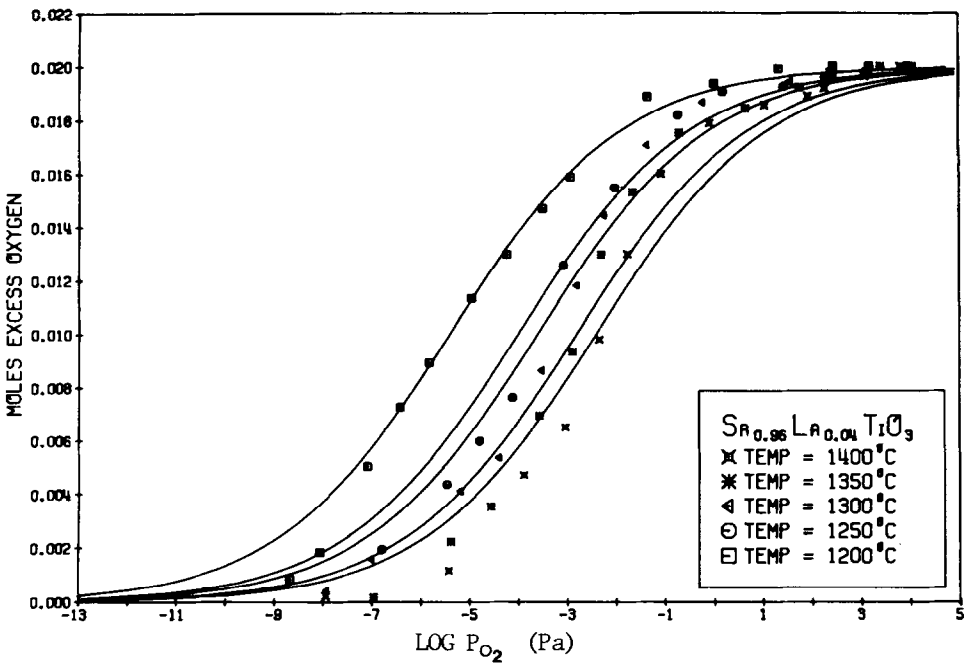

FIG. 1. TGA measurement of excess oxygen absorbed by $Sr_{0.96}La_{0.04}TiO_3$ as function of P_{O_2} in the temperature range 1200 to 1400°C.

Thermogravimetric measurements were made in a TG system designed to measure weight changes on a powder sample, 70–80 g, to an accuracy of ±1 mg (±6 × 10^{-5} mole oxygen). Measurements were conducted at 1000 to 1400°C at an oxygen activity of 10^{-12}–10^{5} Pa, the oxygen activity was monitored by a calibrated zirconia sensor. Details of the apparatus are given elsewhere (*13*).

Electrical conductivity measurements were conducted on porous rectangular bars with four embedded Pt wires welded to Pt leads and attached to a four-terminal digital voltmeter. Conductivity measurements were carried out at 1000–1400°C in an oxygen activity of 10^{-12}–10^{5} Pa.

III. Results and Discussion

Typical TG results are displayed in Figs. 1–4, where the moles of excess or deficit oxygen per mole sample are plotted vs log P_{O_2} as a function of temperature and dopant content. The total amount of oxygen absorbed or evolved is approximately equal to half the total moles of La or Mg present, which implies that full compensation of the dopant is being achieved. No irreversible weight loss was detected for any of the samples within the sensitivity range of the system. The solid curves shown are the values predicted from the proposed models.

Figure 1 illustrates typical results for a *n*-type oxide, $Sr_{0.96}La_{0.04}TiO_3$. As can be seen, to maintain a given level of excess oxygen, higher oxygen activities are required as the temperature increases from 1200 to 1400°C. Figure 2 shows that within our experimental range the amount of excess oxygen absorbed at a given activity is dependent upon the dopant concentration at 1200°C. The equilibrium constant for the oxidation–reduction reaction (Eq. (1)) of donor-doped $SrTiO_3$ is given by

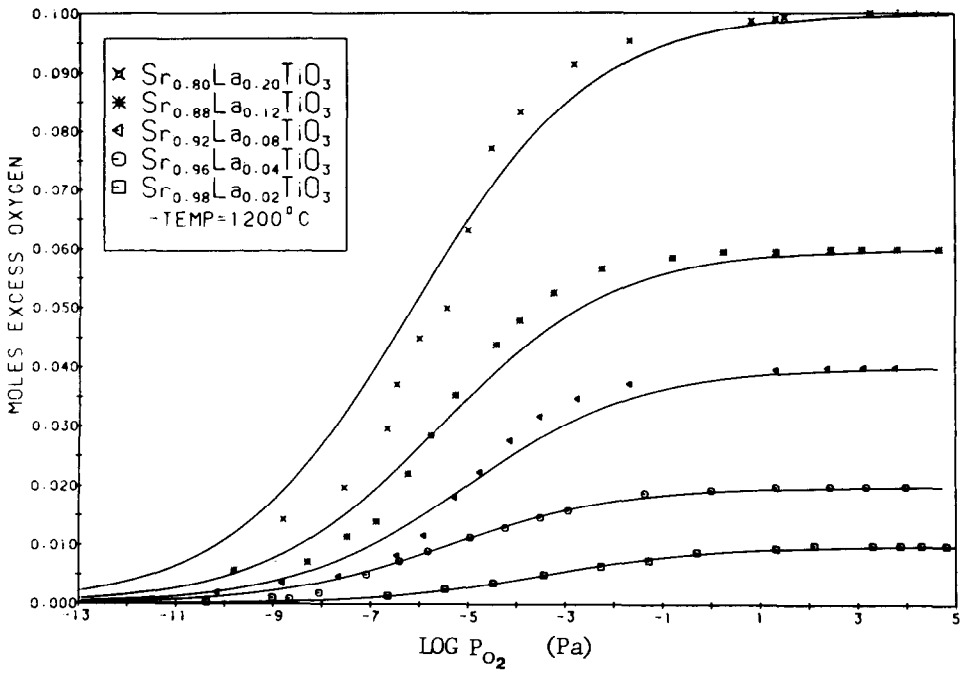

FIG. 2. TGA measurement of excess oxygen absorbed by $Sr_{1-x}La_xTiO_3$ as function of P_{O_2} and La content at 1200°C with x ranging from 0.02 to 0.2.

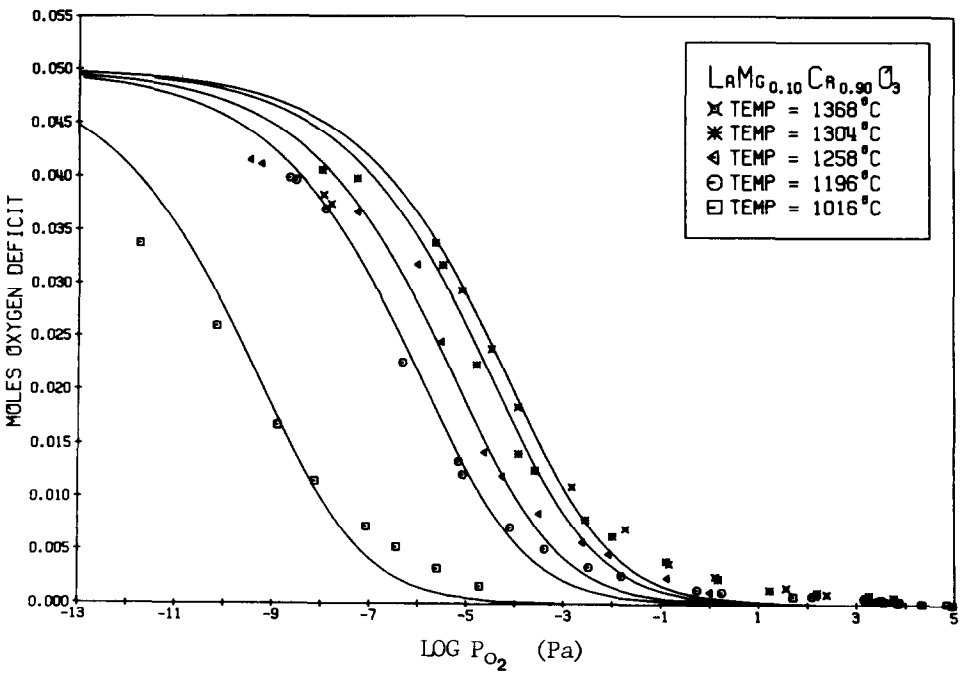

FIG. 3. TGA measurement of oxygen deficit of $LaCr_{0.90}Mg_{0.1}O_3$ as function of P_{O_2} in the temperature range of 1000 to 1400°C.

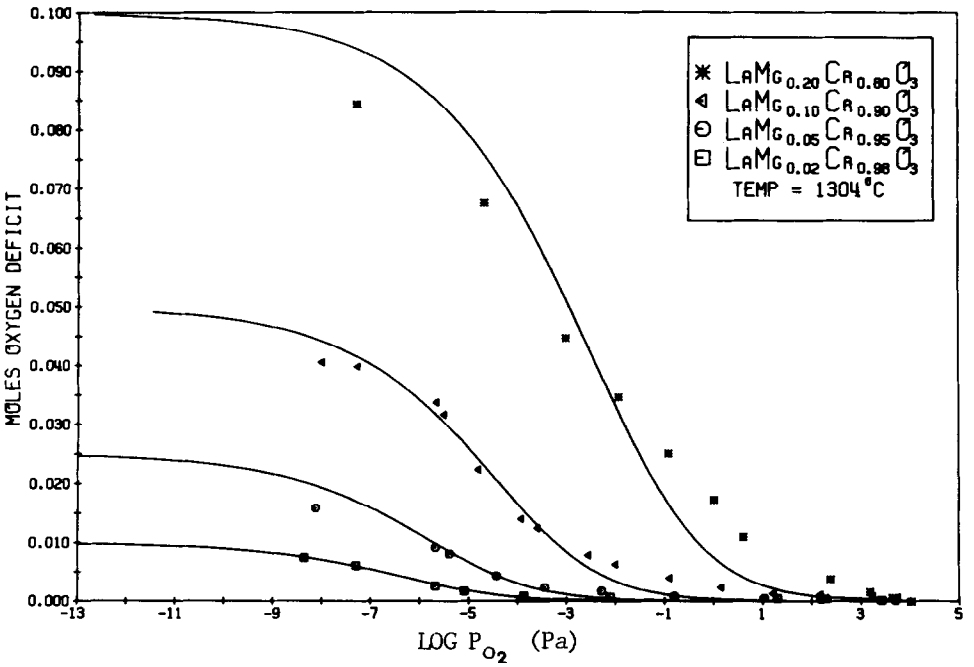

FIG. 4. TGA measurement of oxygen deficit of $LaCr_{1-x}Mg_xO_3$ as function of P_{O_2} and Mg content at 1304°C.

$$K_1 = 1.8 \times 10^6 \exp \frac{(-302 \pm 9 \text{ kJ/mole})}{RT}. \quad (20)$$

Figure 3 illustrates the results obtained for a *p*-type oxide, $LaMg_{0.10}Cr_{0.90}O_3$, equilibrated at temperatures between 1000 and 1368°C. The figure shows that the degree of nonstoichiometry is both temperature and P_{O_2} dependent, it increases with temperature at any given P_{O_2}, furthermore, the same degree of nonstoichiometry is achieved at lower P_{O_2} as the temperature decreases.

The dependence of oxygen deficiency on Mg concentration and P_{O_2} is illustrated in Fig. 4 for data obtained at 1304°C. This figure shows that the degree of nonstoichiometry increases as the amount of dopant increases at any given oxygen activity within the experimental range of 2–20 at.% Mg and 1000 to 1400°C. The equilibrium constant for the oxidation–reduction reaction (Eq. (11)) of acceptor-doped $LaCrO_3$ is accordingly given by

$$K_{11} = 2.1 \times 10^4 \exp \frac{(-272 \pm 16 \text{ kJ/mole})}{RT}. \quad (21)$$

Figures 5 and 6 show that in both donor-doped $SrTiO_3$ and acceptor-doped $LaCrO_3$, the defect concentration and carrier concentration are related to the dopant concentrations in the manner prescribed by Eqs. (8) and (17), respectively. In the case of La CrO_3 deviations are observed for Mg content of 20 at.% Mg. This is probably due to the exsolution of a second phase at about 15 at.% Mg (*14*). In both cases the nonzero intercept at zero dopant concentration appears to be due to impurities.

Figures 7 and 8 illustrate how the major defect and electron concentration change as a function of oxygen activity, temperature, and donor concentrations for a *n*-

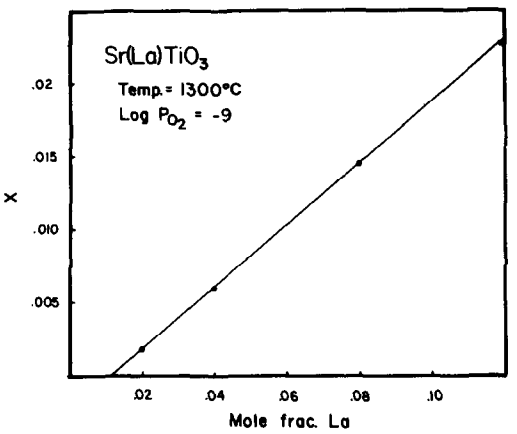

FIG. 5. Excess oxygen concentration as a function of La for $Sr_{1-x}La_xTiO_3$ at 10^{-9} Pa O_2 and 1300°C plotted according to Eq. (8).

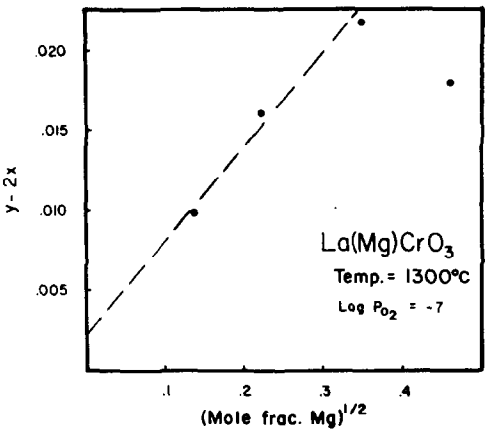

FIG. 6. Carrier concentration of $LaCr_{1-x}Mg_xO_3$, measured by TGA, as function of $[Mg]^{1/2}$ at 10^{-7} Pa and 1300°C plotted according to Eq. (17).

type oxide. To convert the mole fraction values to number of defects or carriers per cubic centimeter, multiply by 1.7×10^{22}. At 1200°C, with a 4 at.% dopant, the maximum conductivity is 25×10^2 S/m. Since the conductivity follows the electron concentration, the value determined for the 4 at.% dopant at 1200°C can be used to estimate the conductivity of $SrTiO_3$ at any temperature and dopant level from Figs. 7 and 8. This approximation is valid because the mobility is only weakly dependent on tem-

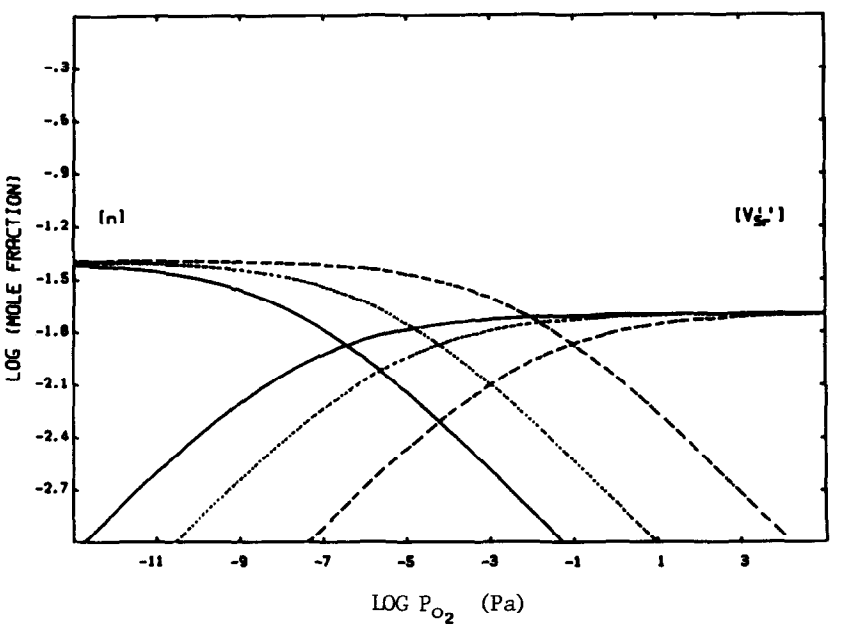

FIG. 7. Major defect and electron concentration as function of P_{O_2} for $Sr_{0.96}La_{0.04}TiO_3$ in the temperature range 1000 to 1300°C, —, 1000°C; ···, 1200°C; – – –, 1300°C.

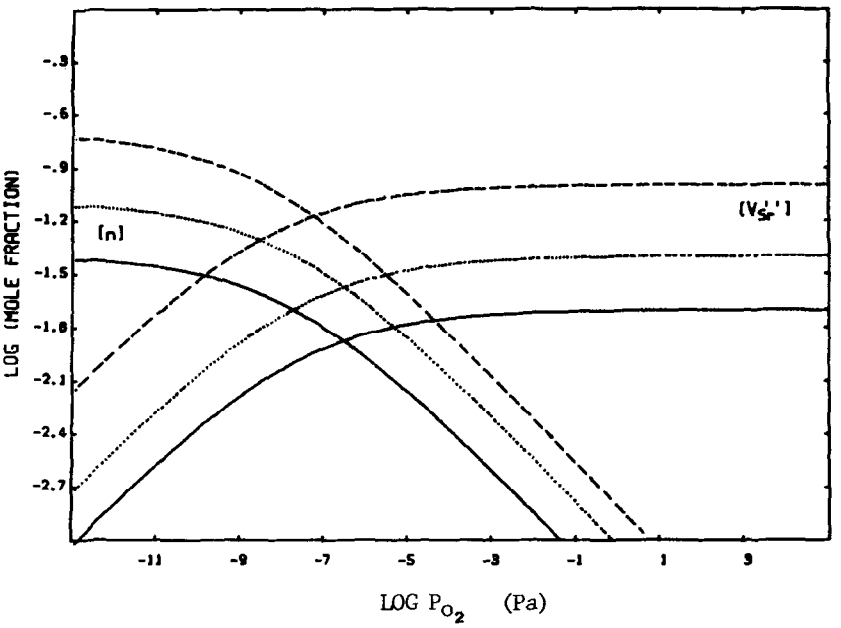

FIG. 8. Major defect and electron concentration of $Sr_{1-x}La_xTiO_3$ as function of P_{O_2} and La content at 1000°C. —, 4 at.% La; ···, 8 at.% La; – – –, 20 at.% La.

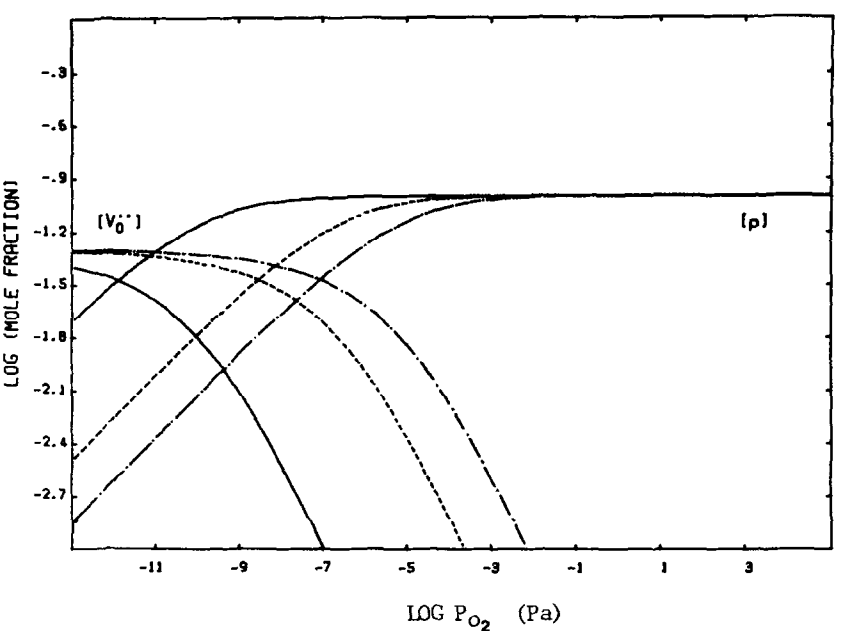

FIG. 9. Major defect and hole concentration as function of P_{O_2} for $LaCr_{0.90}Mg_{0.10}O_3$ in the temperature range 1000 to 1300°C. —, 1000°C; ···, 1200°C; –·–·, 1300°C.

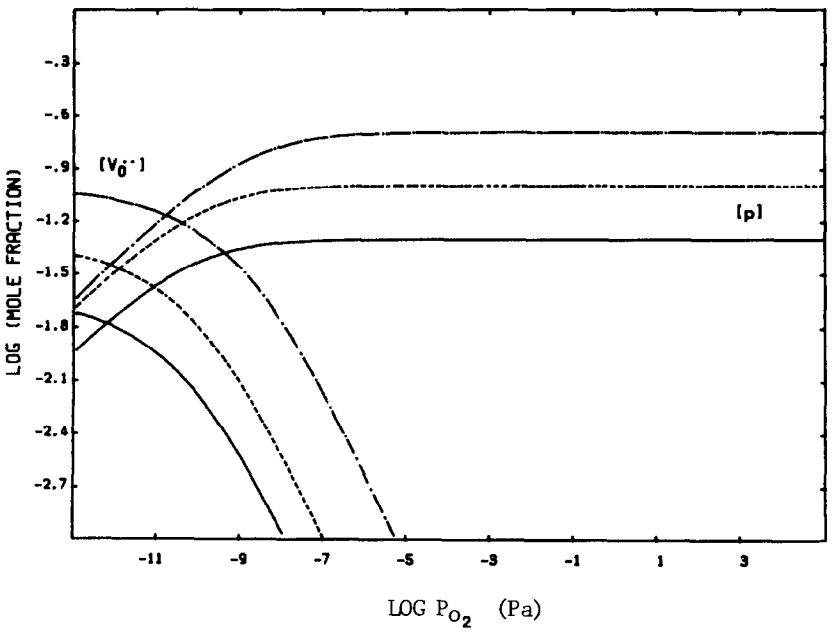

FIG. 10. Major defect and hole concentration of $LaCr_{1-x}Mg_xO_3$ as function of P_{O_2} and La content at 1000°C. —, 5 at.% Mg; · · ·, 10 at.% Mg; —·—, 20 at.% Mg.

perature. For example, for 4 at.% La, at 10^{-11} Pa, the conductivity varies from approximately 25×10^2 at 1200°C to 35×10^2 S/m at 1300°C.

Figures 9 and 10 depict the major defect and hole concentration behavior of a *p*-type oxide as function of acceptor concentration, oxygen activity, and temperature. To convert the mole fraction data to the number of defects, or holes per cubic centimeter, multiply by 1.7×10^{22}.

As was true for *n*-type oxides the electrical conductivity for *p*-type oxides follows the carrier concentration, holes in this instance. The electrical conductivity of Mg-doped $LaCrO_3$ (up to 15 at.% dopant) can be estimated over the entire oxygen activity and temperature range by using the maximum value for a 10 at.% Mg specimen at 1200°C, which is 5×10^2 S/m.

An inspection of Figs. 7 through 10 reveals some rather significant features. In the case of $SrTiO_3$ (*n*-type oxide) the oxygen activity above which the electrical conductivity decreases below 50% of its maximum low oxygen activity value is both La content and temperature dependent. As the temperature increases this point shifts to higher oxygen activity. For example, for 4 at.% La, at 1000°C, this point is 10^{-7} Pa whereas it is 10^{-2} Pa at 1300°C (Fig. 7). As can be seen from Fig. 8, at constant temperature a much weaker dependence on La content is observed. The point shifts slightly to higher oxygen activity as La content decreases. For example, the point shifts only from 10^{-7} to 10^{-6} Pa for 20 and 4 at.% La content, respectively.

Thus, for $SrTiO_3$, the maximum electrical conductivity stability towards oxidation should be expected for the lowest donor dopant concentration operated at the highest temperatures.

In the case of *p*-type oxides, such as $LaCrO_3$, the maximum conductivities are observed at the highest oxygen activities and the P_{O_2} below which greater than 50% decrease in conductivity occur is both compo-

sition and temperature dependent. As was the case for $SrTiO_3$, the dependence on composition is much weaker than that on temperature. As can be seen in Fig. 9, the 50% point shifts from about 10^{-6} to 10^{-11} Pa as temperature decreases from 1300 to 1000°C. In contrast, at 1000°C the 50% point decreases only from 10^{-10} to 10^{-11} as the composition decreases from 20 to 5 at.% mg respectively as shown in Fig. 10.

Accordingly, the maximum electrical stability of $LaCrO_3$ toward reduction can be expected to be achieved for the lowest acceptor content at the lowest temperatures feasible.

IV. Conclusions

The results for the TG and electrical conductivity measurements and defect structure modeling can be summarized as follows:

1. For *n*-type oxides: (a) the maximum electrical conductivity is obtained at the lowest oxygen activities and highest donor concentrations, (b) the maximum oxygen activity at which these oxides can be operated, before the electrical conductivity significantly decreases due to oxidation, is both donor dopant and temperature dependent with the maximum allowable oxygen activities being achieved at the higher temperatures and lower donor contents, e.g., for $Sr_{0.96}La_{0.04}TiO_3$ operated at 1300°C, 10^{-2} Pa is about the maximum useful oxygen activity.

2. For *p*-type oxides: (a) the maximum electrical conductivity is found at the highest oxygen activities, (b) the minimum oxygen activity at which these oxides can operate, before the electrical conductivity significantly decreases due to reduction, is dependent both upon acceptor dopant content and temperature. The minimum operating oxygen activities are achieved by the lower acceptor concentrations and lower temperatures. For example, the minimum useful oxygen activity for $LaCr_{0.95}Mg_{0.05}O_3$ at 1000°C is 10^{-11} Pa as compared to 10^{-6} Pa at 1300°C.

Acknowledgment

This work was supported by the Department of Energy—Grant DEAC0280ER10598A00.

References

1. L. C. Walters and R. E. Grace, *J. Phys. Chem. Solids* **28,** 239 (1967).
2. H. Yamada and G. R. Miller, *J. Solid State Chem.* **6,** 169 (1973).
3. N. H. Chan, R. K. Sharma, and D. M. Smyth, *J. Electrochem. Soc.* **128**(8), 1762 (1981).
4. N. G. Eror and U. Balachandran, *J. Solid State Chem.* **40,** 85 (1981).
5. S. N. Ruddlesdon and P. Popper, *Acta Crystallogr.* **11,** 54 (1958).
6. D. B. Meadowcraft, *in* "Proceedings, Int. Conf. on Strontium-Containing Compounds" (T. Gray, Ed.), p. 119, Atlantic Res. Inst., Halifax, N.S. (1973).
7. D. B. Meadowcraft and J. M. Wimmer, *Ceram. Bull.* **58,** 610 (1979).
8. D. B. Meadowcraft, *Brit. J. Appl. Phys.* **2,** 1225 (1969).
9. H. U. Anderson, *et al.*, "Conference of High Temperature Sciences Related to Open Cycle, Cool-fired MHD Systems," Argonne National Laboratory, April 4–6, 1977, Argonne, Ill.
10. H. U. Anderson, *et al.*, "High Temperature Solid Oxide Fuel Cells," May 5–6, 1977, Brookhaven Nat. Laboratory, Upton, N.Y.
11. I. G. Austin and N. E. Mott, *Adv. Phys.* **18,** 41 (1969).
12. M. Pechini, U.S. Patent 3330697, July 1967.
13. B. Flandermeyer, M.Sc. thesis, University of Missouri-Rolla, 1983.
14. D. Schilling, M.Sc. thesis, University of Missouri-Rolla, 1984.